Biogeosciences
Open Access
Discussions

Space-time dynamics of carbon stocks and environmental parameters related to carbon dioxide emissions in the Buor-Khaya Bay of the Laptev Sea

I. P. Semiletov[1,2], N. E. Shakhova[1,2], I. I. Pipko[2], S. P. Pugach[2], A. N. Charkin[2], O. V. Dudarev[2], D. A. Kosmach[2], and S. Nishino[3]

[1]International Arctic Research Center, University of Alaska Fairbanks, Fairbanks, AK, USA
[2]V. I. Il'ichev Pacific Oceanological Institute, Far Eastern Branch of the Russian Academy of Science, Vladivostok, Russia
[3]Research Institute for Global Change, Japan Agency for Marine-Earth Science and Technology, Yokosuka, Japan

Correspondence to: I. P. Semiletov (igorsm@iarc.uaf.edu)

BGD

10, 2159–2204, 2013

Carbon dynamics in the Buor-Khaya Bay of the Laptev Sea

I. P. Semiletov et al.

Title Page

Abstract	Introduction
Conclusions	References
Tables	Figures

| ⏮ | ⏭ |
| ◀ | ▶ |

Back | Close

Full Screen / Esc

Printer-friendly Version

Interactive Discussion

Abstract

This study aims to improve understanding of carbon cycling in the Buor-Khaya Bay (BKB) by studying the inter-annual, seasonal, and meso-scale variability of carbon stocks and related hydrological and biogeochemical parameters in the water, as well as factors controlling carbon dioxide (CO_2) emission. Here we present data sets obtained on summer cruises and winter expeditions during 12 yr of investigation. Based on data analysis, we suggest that in the heterotrophic BKB area, coastal erosion and river discharge serve as predominant drivers of the organic carbon (OC) cycle, determining OC input and transformation, dynamics of nutrients, carbon stocks in the water column, and atmospheric emissions of CO_2.

1 Introduction

Unlike other oceans, the Arctic Ocean is completely surrounded by permafrost, which is being degraded at an increasing rate under conditions of warming which are most pronounced in Siberia and Alaska (ACIA, 2004; AMAP: SWIPA, 2012). Permafrost underlies a substantial fraction of the Arctic; its thawing accelerates river discharge and carbon losses from soils (Savelieva et al., 2000; Freeman et al., 2001). Thaw and release of organic carbon (OC) from Arctic permafrost is postulated to be one of the most powerful mechanisms causing a net redistribution of carbon from land and ocean to the atmosphere (Gruber et al., 2004; IPCC, 2007; Canadell and Raupach, 2009). Because more than 30 % of the planet's OC storage is in the Arctic region (Tarnocai et al., 2009), remobilization of this carbon and its involvement in the modern biogeochemical cycle was suggested to contribute to the carbon dioxide (CO_2) and methane (CH_4) atmospheric maxima observed above the Arctic (IPCC, 2007; Semiletov et al., 1996; Shakhova et al., 2010a,b; Zimov et al., 1993, 1997). A recent assessment of the carbon balance of Arctic tundra (and boreal forests) shows that Arctic tundra serves as a sink for atmospheric CO_2 (McGuire et al., 2012), while the East Siberian Arctic Shelf

|◀ | ▶|

◀ | ▶

Back | Close

Full Screen / Esc

Printer-friendly Version

Interactive Discussion

(ESAS) was shown to be a source of CO_2 (Semiletov et al., 2007; Semiletov and Pipko, 2007; Pipko et al., 2011). Nevertheless, many gaps still exist in our understanding of the processes responsible for OC transport, transformation, and fate in the Arctic shelf water.

⁵   The East Siberian Arctic Shelf (ESAS) represents a very important part of the Arctic shelf. The ESAS makes up a significant fraction ($\sim 25\%$) of the shelf and holds $> 80\%$ of the Arctic shelf sub-sea permafrost and permafrost-related unique Arctic shelf hydrates (Soloviev, 1987; ACIA, 2004). It accepts about 30% of Arctic river discharge and is surrounded by a coastline that exhibits the highest rates of coastal erosion in ¹⁰ the world (Rachold et al., 2004; Grigoriev et al., 2006; Semiletov et al., 2011, 2012; Vonk, et al., 2012). The ESAS not only responds to the ongoing Arctic warming, but also accommodates the signal of the terrestrial ecosystems' response delivered by Arctic rivers (Guo et al., 2004; Gustafsson et al., 2011; Semiletov et al., 2011). The coastal zone of the ESAS plays the most important role in this response because ¹⁵ incoming river-borne signals and in-situ marine signals first interact in this zone. Processes that develop here include carbon transport, accumulation, and transformation, and seaward export of particulate and dissolved materials to offshore shelf/slope regions (Dudarev et al., 2006; Alling et al., 2010; Sánchez-Garcia et al., 2011; Vonk et al., 2012; Semiletov et al., 2012). In addition, the warming effect of river run-off on the un- ²⁰ derlying sub-sea permafrost also begins in the coastal zone (Semiletov et al., 2011; Nicolsky et al., 2012). Recently reported warming of the shelf water by up to 3 °C and input of riverine waters can accelerate warming of the sub-sea permafrost, causing unsealing of seabed OC deposits (Holemann et al., 2011; Nicolsky et al., 2012).

It the ESAS, it was suggested that carbon cycling is determined by unequal contri- ²⁵ butions of river discharge and coastal erosion, which supply the shelf water with large amounts of terrestrial OC in both particulate and dissolved forms (Gordeev 1996; Lara et al., 1998; Boucsein et al., 2000; Rachold et al., 2000; Stein and Macdonald, 2004; Macdonald et al., 2008; Pipko et al., 2010). Further transformation of terrestrial organic matter (OM), much poorer in nutrients than marine OM, creates a unique aqueous

distribution pattern of biogeochemical parameters and nutrients in the sea water. Analysis of biogeochemical parameters indicative of degradation showed that terrestrial OC was substantially older but less degraded in the surface sediments than in the surface water (Vonk et al., 2010). It has been shown that transformation of coastal erosion-induced OC starts well before it reaches the shelf water (Dudarev et al., 2003). The result of such transformation is the failure of > 50 % of mobilized OC to reach the shelf water due to its release to the atmosphere as CO_2 (Vonk et al., 2012).

The fate of particulate OC (POC) was poorly understood until recently, when it was shown that POC is biologically immobile to a very high degree. Its transformation in shelf water sooner rather than later results in the high partial pressure of CO_2 (pCO_2) observed in the water (Semiletov, 1999a,b; Semiletov et al., 2007, 2011, 2012; Pipko et al., 2005, 2011; Anderson et al., 2009, 2011). After Vonk et al. (2010), it was hypothesized that the yedoma (Ice-Complex)-borne OC, largely associated with mineral-rich matter from coastal erosion, quickly settles to the bottom and exhibits great resistance to degradation. In contrast, young terrestrial OC from surface soil and recent vegetation was found to be more amorphous and humic-like, and lower in density; its buoyancy kept it in the surface water where it became more degraded and, thus, more bioavailable. Finally, it was concluded that yedoma-borne OC and OC from surface soils will contribute differently to the pCO_2 inventory of the Buor-Khaya Bay (BKB) waters (Karlsson et al., 2011). Dissolved OC (DOC) is believed to be brought mainly by rivers and to be relatively inert carbon stock, because its pool turnover time is significantly greater than the shelf water residence time (Dittmar and Kattner, 2003; Alling et al., 2010).

From this point of view, the BKB in the southeastern Laptev Sea is a key site where all these processes interact, determining specific dynamic patterns of hydrological, biogeochemical, and sedimentological parameters observed in the water and water-air interface year-round. Our current contribution aims to share with readers our improved understanding of both OC cycling in this unique area and the factors controlling CO_2 emission, understanding gained through 12 yr of studying the inter-annual, seasonal,

Carbon dynamics in the Buor-Khaya Bay of the Laptev Sea

I. P. Semiletov et al.

Title Page

Abstract | Introduction

Conclusions | References

Tables | Figures

|◀ | ▶|

◀ | ▶

Back | Close

Full Screen / Esc

Printer-friendly Version

Interactive Discussion

and meso-scale variability of carbon stocks and related hydrological and biogeochemical parameters in the BKB water.

2 Data sets and methods

2.1 Study area

⁵ The BKB is located in the southeastern Laptev Sea and is one of the most important Laptev Sea gulfs. It is located between the Lena Delta to the west and Cape Buor-Khaya to the northeast (Fig. 1). The total area of the BKB is about 30 000 km², water depth varies mostly from 10 to 20 m.

The BKB is the primary recipient of Lena River discharge; it receives about 80–90 %
¹⁰ of the river's water and up to 85 % of its sediment discharge (Kassens et al., 1999; Dudarev et al., 2006). The BKB represents a hotspot for erosion input from coastal ice-complexes (called "yedoma" by local people) and was reported to be an important region for land-sea-atmosphere carbon exchanges (Semiletov, 1999a,b; Charkin et al., 2011; Karlsson et al., 2011; Semiletov et al., 2011). Erosion input stems from rapidly
¹⁵ collapsing ice-complexes, which compose up to 30 % of the BKB coastline. Rates of coastal retreat as high as 2–3 m yr⁻¹ were reported within the Lena River Delta (Grigoriev, 1993, 2008) while at some places, e.g. on Muostakh Island which is located roughly in the middle of the gulf, loss by erosion can average 11 m yr⁻¹ (Grigoriev and Kunitsky, 2000, Fig. 2).

²⁰ Hence, the BKB's sedimentary and terrestrial OC material input stems from two major sources: fluvial sediment discharge from the Lena River, and thermal collapse and erosion input from coastal and deltaic ice-complexes (Karlsson et al., 2011). Hydrometeorological conditions, Lena River discharge, and rates of coastal erosion vary inter-annually, creating different backgrounds for the sedimentation processes and OC
²⁵ transport and distribution in the water column and in the surface sediments (Savelieva et al., 2000; Semiletov et al., 2000, 2011; Charkin et al., 2011).

2.2 Materials and methods

Hydrographic observations and sampling were carried out in the southeastern Laptev Sea during the fall seasons of 1999–2000, 2004–2006, 2008–2009, and 2011, and winter seasons of 2002 and 2007 (Table 1).

2.2.1 pH

Seawater samples were collected in Niskin bottles and then transferred into smaller bottles for chemical analysis. pH was determined potentiometrically and reported on the total hydrogen ion concentration scale (DOE, 1994). pH measurement precision was about ±0.004 pH units. Direct comparison between potentiometric and spectrophotometric pH measurements (both on the "total" scale) was carried out in September 2008. Results of this comparison demonstrate good concurrence between the two methods (Pipko et al., 2011). In 2008 the CO_2 system was studied by measuring concentrations of dissolved inorganic carbon (C_T), total alkalinity (A_T), and pH, and computations using the different constituents showed good pH accuracy; C_T and A_T were calibrated versus certified reference materials (CRMs) supplied by Andrew Dickson, Scripps Institution of Oceanography.

2.2.2 A_T

In August-September 2004 and 2005 and in winter 2002 and 2007 A_T was determined as proposed in DOE (1994). The A_T samples were poisoned with a mercuric chloride solution at the time of sampling. Samples were kept in the dark and were analyzed in the lab within one month using an indicator titration method in which 25 mL of seawater was titrated with 0.02 M hydrochloric acid (HCl) in an open cell according to Bruevich (1944). In 2000 the Carbon Dioxide in the Ocean working group of the North Pacific Marine Science Organization (PICES) performed an intercalibration of A_T in seawater using CRMs. The results of the intercalibration showed that the alkalinity values obtained

2164

by the Bruevich method are in agreement with the standard within $\pm 1\,\mu mol\,kg^{-1}$ when state-of-the-art analytical practice is applied (Pavlova et al., 2008).

In August-September 2008 A_T was determined after pH from the same sample on board the *Yakob Smirnitskiy*, using an open-cell potentiometric titration method; 0.05 M HCl was used and the endpoint was determined by a Gran function (Haraldsson et al., 1997). The concentrations thus obtained were calibrated against CRMs. In September 2011 A_T was determined onboard the *Academic Lavrentiev* according to Bruevich (1944), again using CRMs.

The precision of both titration methods was similar at about 0.1 %.

2.2.3 C_T

To measure C_T (fall seasons 1999, 2000) we used a TSVET-530 or LKHM-80MD gas chromatograph (GC), with a Poropac T (1.5 m, 80–120 mesh) and a flame-ionization detector (FID) run isothermally at 30 °C with hydrogen carrier gas; a stripping GC technique similar to that described in Weiss (1981) was used. The total CO_2 (TCO_2) calibrations were based on 0.73, 1.02, and 1.99 mM standard solutions of sodium carbonate (Na_2CO_3) that were prepared gravimetrically in fresh distilled water. Conversion of CO_2 to CH_4 after the Poropac column was done in a nickel (Ni)-catalyst column (14 cm Chromaton, 80–100 mesh, coated with Ni) at 400 °C (Semiletov, 1993). The measurements are reproducible to within ± 1–2 %.

2.2.4   Partial pressure of CO_2

The seawater pCO_2 was computed from pH-A_T using CO2SYS (Lewis and Wallace, 1998), except for cruises in 1999 and 2000 on which the pH-C_T pair was used. The carbonic acid dissociation constants (K_1 and K_2) of Mehrbach et al. (1973) as refit by Dickson and Millero (1987) were used. The uncertainty in computed pCO_2 was about $\pm 10\,\mu atm$.

2.2.5 O$_2$

Dissolved oxygen (O$_2$) concentrations were obtained using a Winkler titration system, giving a precision of $\sim 3\,\mu\mathrm{mol\,kg}^{-1}$ for 1999–2005 data and $\sim 1\,\mu\mathrm{mol\,kg}^{-1}$ for 2008 and 2011 data. These values were then converted to percent saturation, following Weiss (1970).

2.2.6 Nutrients

Nitrates, nitrites, ammonium, silicates, and phosphates were determined by traditional oceanographic techniques prescribed by Ivanenkov and Bordovsky (1978). In September 2008 they were determined by a SmartChem analyzer (http://www.unityscientific. com/products/chem-analyzers-and-sample-prep/smartchem-200.asp). More detailed descriptions can be found elsewhere (Anderson et al., 2009, 2011). The samples were filtered before analysis and evaluated by a 6- to 8-point calibration curve at $\sim 1\,\%$ precision.

2.2.7 Dissolved organic carbon

DOC contents of samples sealed in glass tubes were determined using a Shimadzu TOC-5000 high-temperature catalytic oxidation technique in University of Alaska, Fairbanks laboratories.

2.2.8 Hydrological parameters

During the 2004–2011 cruises a Seabird SBE19plus Profiler (www.seabird.com) was used for measurements of conductivity, temperature, photosynthetically active radiation (PAR) (by LI-193SA Spherical Quantum Sensor), turbidity (by OBS-3 Sensor), and fluorescence. A WetStar fluorimeter was used to assess the in situ colored dissolved OM (CDOM) concentration; this instrument has a single excitation ($E_x = 370$ nm)/emission

($E_m = 460$ nm) wavelength pair. These measurements characterized the distribution of CDOM at 0.20 m vertical intervals at the oceanographic stations.

2.2.9 Analytical methods for sedimentological research

Size composition of fine-grained sediments and suspended particulate matter (SPM) was studied using a laser microanalyzer (Analysette 22, Fritsch GmbH). Sieve analysis was used to examine coarse sediments (Petelin, 1961). Bottom sediment sizing was then performed on the basis of a three-component classification system (Shepard, 1954) that defines sand (1–0.1 mm), silt (0.1–0.01 mm), and clay (< 0.01 mm).

The SPM content was obtained by filtration through membrane filters with pore diameter of 0.47 µm followed by gravimetry. The POC composition was analyzed on samples filtered on pre-combusted (12 h, 450 °C) glass fiber filters (GF/F, 0.7 µm, Whatman), 47 or 142 mm in diameter; after filtration samples were immediately transferred to pre-combusted aluminum envelopes, frozen, and kept at −18 °C until analysis.

Surface sediment samples were retrieved with a Van Veen grab sampler. The topmost surface sediment layer was transferred with stainless steel spatulas to pre-cleaned polyethylene containers before being stored at −18 °C until analysis.

Elementary OC and isotopic (δ^{13}C) composition of bottom sediment were determined by Carlo Erba elemental analyzers and a Finnigan MAT Delta Plus mass spectrometer, respectively, at the International Arctic Research Center, University of Alaska, Fairbanks (USA) and with similar instruments at Stockholm University (Sweden). Accuracy and reproducibility of the isotope results were ±0.1 ‰. Freeze-dried sediments from each station were weighed into pre-combusted silver capsules (5 × 9 mm, Säntis Analytical AG, Teufen, Switzerland), acidified in situ with 50 µL 1 M HCl for removal of carbonates, and dried overnight at 60 °C following a procedure adapted from Gustafsson et al. (1997). A similar procedure of *in situ* acidification and subsequent drying in silver capsules (5 × 12 mm) was followed to measure POC on sub-sampled GF/F (8–12 punches, 5 mm each). Acidified samples were analyzed in triplicate for OC content and δ^{13}C composition using an isotope ratio mass spectrometer.

3   Results and discussion

3.1   Specific features of hydrology, sedimentation, and permafrost dynamics in the BKB

Hydrological conditions in the BKB are determined by Lena River discharge changes,
wind direction and speed, tidal fluctuations of the sea water level, and ice-related con-
ditions. Climatic data show that riverine fresh waters propagate far to the east of the
Lena River Delta (Semiletov et al., 2005). Alteration of the salinity and temperature of
the surface and the bottom shelf water layers depends on the river discharge (Fig. 3)
and prevailing wind conditions (Proshutinsky et al., 1997; Semiletov et al., 2000).

For example, in summer 2005 one of the lowest levels of river discharge (Fig. 3a, b)
in the 1999–2008 period was observed (617 km^3) and winds with average velocities
of 11–12 m s^{-1} prevailed. As a result, the water column in close proximity to the Lena
Delta was mixed to the bottom, while most of the BKB was stratified (Fig. 4a, b). Salinity
varied from 4.9 to 12.1 in the surface layer and from 8.9 to 31.5 in the bottom layer.

In summer 2005 observed temperatures varied from 3.5 to 5.5 °C and from 0.9 to
5 °C, respectively in the surface and bottom layers. In winter 2007, surface and bottom
layer salinities varied from 0.24 to 15.4 and from 0.7 to 27.4, respectively; tempera-
tures ranged from −0.48 to 2.3 °C in the surface layer and from −0.7 to 0.15 °C in the
bottom layer (Fig. 4c, d). In contrast to summer 2005, in summer 2008 the Lena River
discharge was very high (716 km^3) while winds during the period of observations were
mostly low (1–2 m s^{-1}). This resulted in salinity variation from 0.1 to 8.4 in the surface
layer and from 9.3 to 28.9 in the bottom layer (Fig. 4e, f). In summer 2008 temperature
varied from 5.2 to 16.5 °C in the surface water layer and from −1.37 to 7.5 °C in the
bottom water (Fig. 5).

Note that the mean annual Lena River discharge (MAD) observed in the last decade
varied between 617 km^3 and 716 km^3 (Fig. 3a) or ∼ 17–36 % higher than MAD in the
1990 s (∼ 525 km^3). It has been suggested that this reflects a significant increase in the
eastward zonal air water vapor transport from the Northern Atlantic to the Lena River

watershed and increasing shelf-ward transport of permafrost thaw waters observed since the 1990s (Savelieva et al., 2000; Semiletov et al., 2000).

Two different BKB sedimentation regimes were revealed: Type 1 (erosion-accumulation) and Type 2 (accumulation) (Charkin et al., 2011). Under Type 1 accumulation conditions, terrigenous sources of SPM and POC stem predominantly from river discharge and thermal erosion of coastal ice-complexes and remobilized bottom sediments. A Type 1 sedimentation regime occurs more often and is believed to be the quantitatively most important mechanism for SPM and POC delivery to the BKB. According to our data, concentrations of SPM in the near-bottom water layer can reach 187 mg L^{-1} (average 57.9 mg L^{-1}) in the areas where river discharge dominates, and 594 mg L^{-1} in areas located close to the intensively degrading coast. A maximum POC content in bottom waters exceeding 2.0 mg L^{-1} was also observed in the latter areas (Fig. 6a). Note that the mean concentration of SPM observed in the BKB was one order of magnitude greater than the mean concentration of SPM (~ 20 mg L^{-1}) observed along the Lena River stream in summer 2003 (Semiletov et al., 2011).

The Type 2 sedimentation regime usually occurs in winter but can be observed in summer under conditions of halted coastal erosion processes and low river flow or high river discharge associated with gentle winds. For example in 2008, under halted erosion, SPM averaged 2.9 mg L^{-1} in the surface water and 4.8 mg L^{-1} in the bottom water in winter and 11.2 mg L^{-1} in the surface water and 13.4 mg L^{-1} in the bottom water in summer. The POC content did not exceed 0.1 mg L^{-1} in winter (Charkin et al., 2011) and 1.1 mg L^{-1} in summer (Fig. 6).

The water column SPM and POC loadings vary by more than a factor of two between the two regimes. Under the Type 1 sedimentation regime, the highest POC levels were confined to a north-south band east of the delta, in the prodelta, and around Muostakh Island, likely reflecting remobilization of OC from bottom sediments and input of OC from coastal ice complex retreat. Under the Type 2 sedimentation conditions, the highest POC levels were measured in an eastward direction, reflecting river plume propagation from the delta channels to the BKB interior (Charkin et al., 2011).

The δ^{13}C of sea water POC in 2005 ranged from −26.4 to −28.5‰, typical values for both river-borne and coastal erosion-borne POC (Semiletov, 1999a,b; Semiletov et al., 2012; Vonk et al., 2010, 2012), while in 2008, δ^{13}C of POC varied from −24.3‰ to −32.2‰ (Fig. 7); this depletion reflects the strong terrestrial influence of the river plume extending eastward from the Lena Delta.

In winter (April) 2007, when river discharge was significantly smaller but propagated predominantly in the surface water layer, δ^{13}C of surface water POC reflected the river contribution by exhibiting values as depleted as −29.9‰; in the surface sediments the isotopic signature of old terrestrial carbon (from −24.9 to −27.1‰) prevailed, with a small area of much heavier carbon (from −22.2 to −24.0‰) that could be explained by a contribution from sea-ice algae (Charkin et al., 2011).

3.2 Biogeochemical signatures of OC degradation in sea water (dynamics of carbon stocks, nutrients, and related environmental parameters)

Microbial degradation of OM that has been either produced photosynthetically in the euphotic zone or delivered by river and coastal erosion input occurs mostly at the pycnocline and the water-sediment interface, which results in decreasing O_2 concentrations, increasing nutrients concentrations (primarily phosphate, PO_4^{3-}, and nitrate, NO_3^-), and increasing pCO$_2$ in the bottom water. In the ESAS, the total amount of OC is the sum of primarily produced OC, OC delivered to the shelf water by river runoff, and OC resulting from coastal and bottom erosion (Stein and Macdonald, 2004; Semiletov et al., 2011, 2012). This pool consists of two major carbon stocks: POC and DOC. POC represents an earlier phase of OM transformation associated with poorly-defined compositional changes such as aggregation/disaggregation of particles, incorporation of older and more degraded material, and recombination of organic compounds (Cooper et al., 2005). In the BKB, major POC sources include soil and yedoma-borne terrestrial OC and OC mobilized to the water column by coastal and bottom erosion (Vonk et al., 2010, 2012; Karlsson et al., 2011).

Full Screen / Esc

Printer-friendly Version

Interactive Discussion

Riverine DOC inputs were long considered recalcitrant because of their high C : N ratio (~ 50), the predominance of high molecular weight (HMW) compounds, and the relatively low degree of mixing observed in the estuaries (Mantoura and Woodward, 1983; Amon and Benner, 1996). Nevertheless, it was recently shown that not all of the

5   HMW DOC pool is refractory. About 17 % of the DOC was reported to be biologically available in lake, river, and marine ecosystems (Sondergaard and Middelboe, 1995). To be incorporated into the microbial food web, large DOC molecules might be broken by sunlight into smaller and potentially more labile entities (Jørgensen et al., 1998; Wiegner and Seitzinger, 2001). Measurements of DOC are very labor-intensive and

10   not always possible during cruises. At the same time, the fraction of DOC that is colored (CDOM) exhibits very strong positive correlation with fluorescence; it can easily be measured in-situ using a WETStart fluorometer (Belzile et al., 2006). In the ESAS, CDOM is colored because riverine runoff is loaded with humic acids, which are representative of Arctic/Subarctic carbon cycling. Note that satellite data available for the

15   ESAS often treat CDOM, incorrectly, as a fraction of ocean-color-derived Chl *a*, resulting in an overestimation of primary production rates by an order of magnitude (Heim et al., 2013). In our previous studies, we found a strong positive correlation between river-borne DOC and CDOM (Semiletov et al., 2007; Shakhova and Semiletov, 2008; Pugach and Pipko, 2013), which allowed us to further treat CDOM as a parameter

20   indicative of riverine DOC.

Below we present more detailed analyses of the relationship between CDOM, POC, water salinity, $p\text{CO}_2$, and NO_3^- and PO_4^{3-} concentrations measured in the BKB water column in summer 2005 (Fig. 8) and 2011 (Fig. 9 and Fig. 10) and winter 2002 and 2007 (Fig. 11).

25   From Fig. 8a, it can be seen that in 2005 POC concentrations in the water column along the transect varied from $0.1\,\text{mg L}^{-1}$ to $0.4\,\text{mg L}^{-1}$. Higher POC concentrations were associated equally with water of higher salinity and with water of lower salinity, while higher CDOM concentrations, indicative of DOC, largely corresponded to low-salinity water. This implies that river runoff served as a source of DOC to the BKB.

pCO$_2$ along the transect ranged from a few hundreds to 4000 µatm, which implies supersaturation by up to 10 times relative to equilibrium with atmosphere. Higher pCO$_2$ values were observed where salinity and POC levels were higher and CDOM was lower, suggesting that the predominant source of CO$_2$ in the water column is not river runoff (Fig. 8b, e). We also found that when POC concentrations in waters of different salinities were comparable, higher pCO$_2$ occurred where salinity was higher (Fig. 8c). NO$_3^-$ concentrations in the water column along the transect varied from negligible values up to 8 mg L^{-1}. Higher NO$_3^-$ concentrations were observed in saltier water and were associated with lower CDOM concentrations, which suggests that coastal erosion, rather than river runoff, is the NO$_3^-$ source (Fig. 8f). In 2011, relationships between studied parameters were similar to those observed in 2005 except for levels of pCO$_2$ detected in the water column (Fig. 9).

In summer 2011, sea water pCO$_2$ varied from near saturated relative to the atmosphere ($\sim$ 400 µatm) to 2.5 times oversaturated (900 µatm), much lower than in summer 2005, when sea water oversaturation reached 10 times relative to atmosphere. Note that the 2005 Lena River discharge was the lowest in the last ten years, while in 2011 it was about average volume. Because concentrations of nutrients (NO$_3^-$, Fig. 9a, b) in 2005 and in 2011 were comparable, we suggest that rates of OM degradation were also comparable. That implies that the observed difference in pCO$_2$ between the two years was caused by strong 2011 winds (10–20 m s^{-1}) which induced higher levels of coastal erosion and wind-driven surface sediment resuspension (Heim et al., 2013) that contributed to the OM supply to the shelf water. At the same time more frequent and longer-lasting storms caused intense water mixing down to the very bottom and consequent release of CO$_2$ to the atmosphere, allowing significant unloading of the water column CO$_2$ (Fig. 10). In the winter, when the Lena River discharge was up to 10 times less than in summer (Fig. 3b), values of pCO$_2$ in the water column remained comparable with those observed in summer 2005 (up to 4000 µatm, Fig. 11a, d).

As is clearly seen in Fig. 11, in winter the highest pCO$_2$ values were associated with bottom water and could be attributed to the microbial degradation of OM that occurs

Full Screen / Esc

Printer-friendly Version

Interactive Discussion

at the water-sediment interface. Because the water column is better stratified in winter, vertical distribution of $p\mathrm{CO_2}$ in the water column reflected the stratification pattern. Because the BKB in winter is covered with sea ice, $\mathrm{CO_2}$ release to the atmosphere is restricted, which allows accumulation of $p\mathrm{CO_2}$ up to 5000 µatm (Semiletov et al., 2004), higher than $p\mathrm{CO_2}$ values measured in winter (1267–1579 µatm) in the Lena Delta channels (Semiletov et al., 2011).

Degradation of the OC resulting in increasing $p\mathrm{CO_2}$ is manifested by decreasing concentrations of $\mathrm{O_2}$. As is seen in Fig. 12a, the most pronounced increase in $p\mathrm{CO_2}$ corresponded with a decrease in concentrations of $\mathrm{O_2}$ in the bottom water, where the highest $p\mathrm{CO_2}$ and the lowest levels of $\mathrm{O_2}$ were observed. Higher $p\mathrm{CO_2}$ in the bottom water resulted in lower pH or an acidified water column (Fig. 12b). The strong negative correlation observed between salinity and pH ($R = -0.82$, $n = 43$ in 2005) implies that coastal erosion/oxidation of eroded OM rather than river discharge is responsible for acidifying shelf water (Table 2). Intensive water mixing weakened the correlation to $R = -0.43$, $n = 74$ in 2011 as was described above.

We observed strong negative correlation between $p\mathrm{CO_2}$ and $\mathrm{O_2}$ ($R = -0.97$, $n = 43$ in 2005 and $R = -0.92$, $n = 74$ in 2011), between $\mathrm{O_2}$ and $\mathrm{NO_3^-}$ ($R = -0.87$, $n = 43$ in 2005 and $R = -0.84$, $n = 74$ in 2011), and between $\mathrm{O_2}$ and $\mathrm{PO_4^{3-}}$ ($R = -0.7$, $n = 43$ in 2005 and $R = -0.84$, $n = 74$ in 2011). We found a strong positive correlation between $p\mathrm{CO_2}$ and $\mathrm{NO_3^-}$ ($R = 0.75$, $n = 43$ in 2005 and $R = 0.91$, $n = 74$ in 2011), and between $p\mathrm{CO_2}$ and $\mathrm{PO_4^{3-}}$ ($R = 0.53$, $n = 43$ in 2005 and $R = 0.83$, $n = 74$ in 2011) (Table 2 and Table 3) suggesting that high $p\mathrm{CO_2}$ is caused by in situ microbial OM (POC) decomposition in the water column.

Our data show that concentrations of nutrients ($\mathrm{NO_3^-}$ in the range of 5 to 8 µM and $\mathrm{PO_4^{3-}}$ in the range of 0.45 to 1.45 µM) observed in the water column near Buor-Khaya Cape, known to be a landform subject to very high rates of coastal erosion, were significantly greater than values measured in the Lena River. Specifically, in the Lena River, $\mathrm{NO_3^-}$ concentrations ranged from 0.01 to 1.4 µM, and $\mathrm{PO_4^{3-}}$ concentrations ranged from

0.2 to 1.0 µM (Lara et al., 1998). The vertical distribution of nutrients (NO_3^-, PO_4^{3-}), pCO_2, and oxygen saturation in the BKB area, as seen in Fig. 13, also demonstrate that degradation of the eroded terrestrial OM rather than river-transported OM serves as the predominant source of nutrients in the BKB.

High rates of nutrients in the Lena River water column imply high primary production potential in the euphotic layer. Nevertheless, it was reported that primary production in the BKB was higher (75 to 640 mg C m^{-2} day^{-1})than in the Lena River/Delta (50 to only 160 mg C m^{-2} day^{-1}), but was limited by low water transparency caused by the extremely high water turbidity (Sorokin and Sorokin, 1996). Another reason for the low transparency/primary production could be high CDOM values; values are one order of magnitude higher in the Lena River (up to 100–110 mg m^{-3}), in the Laptev Sea (up to 50–70 mg m^{-3}), and in the western part of the East Siberian Sea (> 30 mg m^{-3}) than in the eastern part of the East Siberian Sea (5 mg m^{-3}). This is because the Laptev Sea and the western East Siberian Sea are strongly influenced by riverine runoff enriched in humic substances (Semiletov et al., 2005, 2007; Pugach and Pipko, 2013). Low transparencies are reflected by in-situ Secchi depths of less than 0.5 m near the Bykovsky channel outlet (in summer 2008, by Heim et al., 2013) and 0.2–0.4 m in Neelov Bay and the Bykovsky channel (summer 2003, authors' data).

These data are important to take into consideration while evaluating the satellite data. Based on satellite data, it was concluded that increases in net primary production (NPP) occurred in the eastern Arctic Ocean over the 12 yr study period (1998 to 2009). The largest increase in NPP in the eastern Arctic Ocean observed between 1998 and 2009 was reported in the oligotrophic Siberian shelf (from 101 ± 15.8 in the Siberian sector to 121 ± 20.2 g C m^{-2} yr^{-1} in the Laptev, or +135 %) (Arrigo and van Dijken, 2011). At the same time, in the most productive western sector, NPP was reported from 71.3 ± 11.0 g C m^{-2} yr^{-1} in the Beaufort to 96.9 ± 7.4 g C m^{-2} yr^{-1} in the Chukchi seas. Nevertheless, field data show that NPP in the highly productive Chukchi Sea is one to two orders of magnitude higher (up to 200–400 g C m^{-2} yr^{-1}) than in the oligotrophic Laptev Sea and western part of the East Siberian Sea (Walsh et al., 1989;

Sorokin and Sorokin, 1996). Thus, the proposed NPP increase based on interpretation of satellite data must be validated with observational data (Heim et al., 2013). Meanwhile, the observed increase in the Lena River discharge of up to 37 % since the 1990 s suggests that increased levels of annual primary production could be explained by an increasing load of humic acids delivered to shelf water; in this water the color from CDOM mimics the color from Chl a as seen from space.

3.3 BKB and its coastal zone as a source of CO_2 emissions to the atmosphere

The multi-year investigation of BKB pCO_2 shows that strong oversaturation of the surface water predominantly occurred in the eastern part of the study area (Fig. 14), while sometimes a slight oversaturation ($\sim 400\,\mu$atm) was observed in the small area adjacent to the Lena River Delta, perhaps as a result of lower pCO_2 values in the river water followed by the enhanced uptake of CO_2 by photosynthesis (Sorokin and Sorokin, 1996).

The result of surface water oversaturation with CO_2 is that surface water serves as a source of CO_2 to the atmosphere. As is shown in Fig. 15, the BKB surface is a source of CO_2 to the atmosphere with rates varying from near zero to $56\,\mathrm{mM\,m^{-2}\,day^{-1}}$ in 2005, and from near zero to $95\,\mathrm{mM\,m^{-2}\,day^{-1}}$ in 1999. In winter pCO_2 remained high, exceeding the summer values, due to restricted ventilation of the ice-covered water column (Semiletov et al., 2004, 2007). The bottom water is oversaturated with CO_2 year-round and the potential exists for the CO_2 to be released into the atmosphere through open flaw polynyas because of deep convection (Shakhova et al., 2010a).

It was reported that the area surrounding Muostakh Island experiences coastal erosion of up to 15–20 m during only a few summertime weeks, much higher than the average coastal erosion rates in the area (Grigoriev and Kunitsky, 2000). A significant fraction of old carbon activated by erosion of coastal permafrost is released directly to the atmosphere as CO_2 as a result of sub-aerial degradation (Vonk et al., 2012), in contrast to the prior assumption that all thawed and erosion-mobilized OC is flushed into

Full Screen / Esc

Printer-friendly Version

Interactive Discussion

the sea (Stein and Macdonald, 2004). Figure 16 presents observational data on CO_2 emissions from the thawing ice-complex measured by the same technique in September 2006 and September 2009 along similar transects across the Northern Cape of Muostakh Island.

As seen in Fig. 16, the CO_2 fluxes measured in late September 2009 were in the same range (6–319 mM m^{-2} day^{-1}) as fluxes measured in early September 2006 (3–439 mM m^{-2} day^{-1}, Vonk et al., 2012). These fluxes were a few-fold greater than those observed from the tundra (8.6–9.5 mM m^{-2} day^{-1}) on the neighboring Primorsky coastal plain. The CO_2 fluxes measured at near-shore sites were much lower than those observed from the beach but were in the range of CO_2 fluxes (1–50 mM m^{-2} day^{-1}) reported for other shallow areas of the ESAS impacted by export of eroded carbon (Pipko et al., 2011; Semiletov et al., 2011, 2012). In terms of inter-annual variability, CO_2 fluxes observed at sea sites in September 2009 (34–41 mM m^{-2} day^{-1}) were slightly higher than in September 2006 (26–34 mM m^{-2} day^{-1}).

4 Conclusions

Based on our multi-year data (1999–2011), we suggest that in the BKB, heterotrophic processes associated with river discharge and coastal erosion drive OC input and transformation, dynamics of nutrients, and carbon stocks in the water column. Specifically:

– Input of terrestrially-borne OC varies seasonally and inter-annually and is largely determined by rates of coastal erosion and river discharge. The latter has increased during the last two decades by up to 36 %.

– Hydrological conditions in the BKB reflect ongoing changes in river runoff, which have resulted in fresher and warmer water observed in summer and winter.

- The sedimentation regime in the BKB changes from erosion-accumulation (Type 1) to accumulation (Type 2). Loadings of the water column with particulate material vary by more than a factor of two between the two regimes.

- Higher levels of pCO_2, higher concentrations of nutrients, and lower levels of oxygen saturation were observed in the bottom water near the eroded coasts; this implies that coastal erosion and subsequent oxidation of eroded OM rather than the Lena River serves as the predominant source of nutrients to the BKB.

- CO_2 fluxes from the BKB and ESAS sea water (1–$50\,\mathrm{mM\,m^{-2}\,day^{-1}}$) into the atmosphere are determined by specific features of hydrology and wind conditions, which change seasonally and inter-annually; this implies that the sea surface is a more significant source of CO_2 to the atmosphere than the tundra (see below).

- Atmospheric CO_2 emissions (3–$439\,\mathrm{mM\,m^{-2}\,day^{-1}}$) measured from a thawed ice-complex in the BKB in two years (2006 and 2009) suggest that the coastal area serves as a more significant source of CO_2 to the atmosphere than the tundra (8.6–$9.5\,\mathrm{mM\,m^{-2}\,day^{-1}}$) on the neighboring Primorsky coastal plain.

The BKB area can be employed as an integrator of ongoing changes in the surrounding environment. These changes create a terrestrial or exogenous signal generated by increasing coastal and bottom erosion (increasing export of terrestrial POC to the Arctic Ocean), increasing river runoff (increasing export of terrestrial DOC/humic acids/CDOM to the Arctic Ocean), and involvement of terrestrial carbon in the modern biogeochemical cycle. Thus, we suggest that under ongoing changes, more nutrients, products of eroded OC transformation and river transport, will be delivered to the Arctic Ocean with its shrinking ice cover, potentially increasing primary production outside of the shallow ESAS. At the same time, because the ESAS is characterized by very low transparency which limits thickness of the euphotic layer, excessive pCO_2 will not be utilized by photosynthesis, but will rather be emitted to the atmosphere at increasing rates affecting regional CO_2 balance.

References

ACIA: Impacts of a Warming Arctic: Arctic Climate Impact Assessment, Cambridge University Press, Cambridge, 139 pp., 2004.

Alling, V., Sánchez-García, L., Porcelli, D., Pugach, S., Vonk, J., van Dongen, B., Mörth, C. M., Anderson, L. G., Sokolov, A., Andersson, P., Humborg, C., Semiletov, I., and Gustafsson, Ö.: Nonconservative behavior of dissolved organic carbon across the Laptev and East Siberian seas, Global Biogeochem. Cy., 24, GB4033, doi:10.1029/2010GB003834, 2010.

AMAP: Snow, Water, Ice and Permafrost in the Arctic (SWIPA): Climate Change and the Cryosphere, Arctic Monitoring and Assessment Programme (AMAP), Oslo, Norway, 538 pp., 2012.

Amon, R. M. W. and Benner, R.: Bacterial utilization of different size classes of dissolved organic matter, Limnol. Oceanogr., 41, 41–51, 1996.

Anderson, L. G., Jutterström, S., Hjalmarsson, S., Wahlström, I., and Semiletov, I.: Out-gassing of CO_2 from Siberian Shelf seas by terrestrial organic matter decomposition, Geophys. Res. Lett., 36, L20601, doi:10.1029/2009GL040046, 2009.

Anderson, L. G., Björk, G., Jutterström, S., Pipko, I., Shakhova, N., Semiletov, I., and Wåhlström, I.: East Siberian Sea, an Arctic region of very high biogeochemical activity, Biogeosciences, 8, 1745–1754, doi:10.5194/bg-8-1745-2011, 2011.

Arrigo, K. R. and van Dijken, G.: Secular trends in Arctic Ocean net primary production, J. Geophys. Res., 116, C09011, doi:10.1029/2011JC007151, 2011.

Belzil, C. C., Roesler, S., Christensen, J. P., Shakhova, N., and Semiletov, I.: Fluorescence measured using the WETStar DOM fluorometer as a proxy for dissolved matter absorption, Estuar. Coast. Shelf Sci., 67, 41–49, 2006.

Boucsein, B., Fahl, K., and Stein, R.: Variability of river discharge and Atlantic-water inflow at the Laptev Sea continental margin during the past 15,000 yr: implications from maceral and biomarker records, Int. J. Earth Sci., 89, 578–591, 2000.

Bruevich, S. V.: Instruction for Chemical Investigation of Seawater, Glavsevmorput, Moscow, 83 pp., 1944 (in Russian).

Canadell, J. G. and Raupach, M. R.: Land carbon cycle feedbacks, in: Arctic Climate Feedbacks: Global Implications, edited by: Sommerkorn, M. and Hassol, S. J., WWF International Arctic Programme, Oslo, 70–80, 2009.

Charkin, A. N., Dudarev, O. V., Semiletov, I. P., Kruhmalev, A. V., Vonk, J. E., Sánchez-García, L., Karlsson, E., and Gustafsson, Ö.: Seasonal and interannual variability of sedimentation and organic matter distribution in the Buor-Khaya Gulf: the primary recipient of input from Lena River and coastal erosion in the southeast Laptev Sea, Biogeosciences, 8, 2581–2594, doi:10.5194/bg-8-2581-2011, 2011.

Dickson, A. G. and Millero, F. J.: A comparison of the equilibrium constants for the dissociation of carbonic acid in seawater media, Deep-Sea Res., 34, 1733–1743, 1987.

Dittmar, T. and Kattner, G.: The biogeochemistry of the river and shelf ecosystem of the Arctic Ocean: a review, Mar. Chem., 83, 103–120, 2003.

DOE: Handbook of Methods for the Analysis of the Various Parameters of the Carbon Dioxide System in Sea Water, Version 2, edited by: Dickson, A. G. and Goyet, C., 1994.

Dudarev, O., Semiletov, I., Botsul, A., and Charkin, A.: Modern sedimentation in the coastal cryolithozone of the Dmitry Laptev Strait/East-Siberian Sea, Pacific Geology, 22, 51–60, 2003 (translated into English).

Dudarev, O. V., Semiletov, I. P., and Charkin, A. N.: Particulate material composition in the Lena River-Laptev Sea system: scales of heterogeneities, Dokl. Earth Sci., 411A, 1445–1451, 2006 (translated in English).

Freeman, C., Evans, C. D., Monteith, D. T., Reynolds, B., and Fenner, N.: Export of organic carbon from peat soils, Nature, 412, 785, doi:10.1038/35090628, 2001.

Gordeev, V. V., Martin, J. M., Sidorov, I. S., and Sidorova, M. V.: A reassessment of the Eurasian river input of water, sediment, major elements, and nutrients to the Arctic Ocean, Am. J. Sci., 296, 664–691, 1996.

Carbon dynamics in the Buor-Khaya Bay of the Laptev Sea

I. P. Semiletov et al.

Title Page

Abstract | Introduction

Conclusions | References

Tables | Figures

◀ | ▶

◀ | ▶

Back | Close

Full Screen / Esc

Printer-friendly Version

Interactive Discussion

Grigoriev, M. N.: Criomorphogenesis of the Mouth Area of the Lena River, Institute of Permafrost Study of the Siberian Branch of the Russian Academy of Science, Yakutsk, 1–176, 1993 (in Russian).

Grigoriev, M. N.: Cryomorphogenesis and Lithodynamics of the Coastal-Shelf Zone of the Seas of Eastern Siberia, Doctoral thesis, Melnikov Permafrost Inst., Yakutsk, 2008 (in Russian).

Grigoriev, M. N. and Kunitsky, V. V.: Destruction of the sea coastal ice-complex in Yakutia, in: Hydrometeorological and Biogeochemical Research in the Arctic, Proc. Arctic Regional Center, 2, edited by: Semiletov, I. P., Dal'nauka Press, Vladivostok, 109–116, 2000 (in Russian).

Grigoriev, M. N., Razumov, S. O., Kunitzkiy, V. V., and Spektor, V. B.: Dynamics of the Russian East Arctic Sea coast: major factors, regularities and tendencies, Earth's Cryosphere, X(4), 74–94, 2006 (in Russian).

Gruber, N., Friedlingstein, P., Field, C. B., Valentini, R., Heimann, M., Richey, C. B., Romero-Lankao, P., Schulze, D., and Chen, C.-T. A.: The vulnerability of the carbon cycle in the 21st century: an assessment of carbon-climate-human interactions, in: The Global Carbon Cycle: Integrating Humans, Climate, and the Natural World, edited by: Field, C. B. and Raupach, M. R., Island Press, Washington DC, 45–76, 2004.

Guo, L., Semiletov, I., Gustafsson, Ö., Ingri, J., Andersson, P., Dudarev, O., and White, D.: Characterization of Siberian Arctic coastal sediments: implications for terrestrial organic carbon export, Global Biogeochem. Cy., 18, GB1036, doi:10.1029/2003GB002087, 2004.

Gustafsson, Ö., Haghseta, F., Chan, C., MacFarlane, J., and Gschwend, P. M.: Quantification of the dilute sedimentary soot phase: implications for PAH speciation and bioavailability, Environ. Sci. Technol., 31, 203–209, 1997.

Gustafsson, Ö., van Dongen, B. E., Vonk, J. E., Dudarev, O. V., and Semiletov, I. P.: Widespread release of old carbon across the Siberian Arctic echoed by its large rivers, Biogeosciences, 8, 1737–1743, doi:10.5194/bg-8-1737-2011, 2011.

Haraldsson, C., Anderson, L. G., Hassellov, M., Hulth, S., and Olsson, K.: Rapid, high-precision potentiometric titration of alkalinity in ocean and sediment pore waters, Deep-Sea Res. Pt. I, 44, 2031–2044, 1997.

Heim, B., Abramova, E, Doerffer, R, Guenther, F., Holemann, J., Kraberg, A., Lantuit, H., Loginova, A., Martynov, F., Overduin, P. P., and Wegner, C.: Ocean color remote sensing in the Southern Laptev Sea: evaluation and applications, Biogeosciences Discuss., accepted, 2013.

Title Page

Abstract | Introduction

Conclusions | References

Tables | Figures

|◄ | ►|

◄ | ►

Back | Close

Full Screen / Esc

Printer-friendly Version

Interactive Discussion

Holemann, J., Kirillov, S., Klagge, T., Novikhin, A., Kassens, H., and Timokhov, L.: Near-bottom water warming in the Laptev Sea in response to atmospheric sea-ice conditions in 2007, Polar Res., 30, 6425–6440, 2011.

IPCC: Climate Change 2007: The Physical Science Basis. Contribution of Working Group I to the Fourth Assessment Report of the Intergovernmental Panel on Climate Change, edited by: Solomon, S., Qin, D., Manning, M., Chen, Z., Marquis, M., Avery, K. B., Tignor, M., and Miller, H. L., Cambridge University Press, Cambridge, UK and NY, NY, USA, 996 pp., 2007.

Ivanenkov, V. N. and Bordovsky, O. K.: Methods of Hydrochemical Investigation of Seawater, Nauka, Moscow, 270 pp., 1978 (in Russian).

Jørgensen, N. O. G., Tranvik, L., Edling, H., Granéli, W., and Lindell, M.: Effects of sunlight on occurrence and bacterial turnover of specific carbon and nitrogen compounds in lake water, FEMS Microbiol. Ecol., 25, 217–227, 1998.

Karlsson, E. S., Charkin, A., Dudarev, O., Semiletov, I., Vonk, J. E., Sánchez-García, L., Andersson, A., and Gustafsson, Ö.: Carbon isotopes and lipid biomarker investigation of sources, transport and degradation of terrestrial organic matter in the Buor-Khaya Bay, SE Laptev Sea, Biogeosciences, 8, 1865–1879, doi:10.5194/bg-8-1865-2011, 2011.

Kassens, H., Bauch, H. A., Dmitrenko, J. A., Eicken, H., Hubberten, H. W., Melles, M., Thiede, J., and Timokhov, L. A.: Land-Ocean Systems in the Siberian Arctic: Dynamics and History, Springer, Berlin, Heidelberg, New York, 711 pp., 1999.

Lara, R. J., Rachold, V., Kattner, G., Hubberten, H.-W., Guggenbergen, G., Skoog, A., and Thomas, D. N.: Dissolved organic matter and nutrients in the Lena River, Siberian Arctic: characteristics and distribution, Mar. Chem., 59, 301–309, 1998.

Lewis, E. and Wallace, D. W. R.: Program developed for CO_2 system calculations, ORNL/CDIAC-105, Carbon Dioxide Information Analysis Center, Oak Ridge National Laboratory, US Department of Energy, Oak Ridge, Tennessee, 1998.

Macdonald, R. W., Anderson, L. G., Christensen, J. P., Miller, L. A., Semiletov, I. P., and Stein, R.: The Arctic Ocean: budgets and fluxes, carbon and nutrient fluxes, in: Continental Margins: A Global Synthesis, edited by: Liu, K.-K., Atkinson, L., Quinones, R., and Talaue-McManus, L., Springer, Berlin, 291–303, 2008.

Mantoura, R. F. C. and Woodward, E. M. S.: Conservative behavior of riverine dissolved organic-carbon in the Severn Estuary – chemical and geochemical implications, Geochim. Cosmochim. Acta, 47, 1293–1309, 1983.

Carbon dynamics in the Buor-Khaya Bay of the Laptev Sea

I. P. Semiletov et al.

Title Page

Abstract	Introduction
Conclusions	References
Tables	Figures

|◄ | ►|

◄ | ►

Back | Close

Full Screen / Esc

Printer-friendly Version

Interactive Discussion

McGuire, A. D., Christensen, T. R., Hayes, D., Heroult, A., Euskirchen, E., Kimball, J. S., Koven, C., Lafleur, P., Miller, P. A., Oechel, W., Peylin, P., Williams, M., and Yi, Y.: An assessment of the carbon balance of Arctic tundra: comparisons among observations, process models, and atmospheric inversions, Biogeosciences, 9, 3185–3204, doi:10.5194/bg-9-3185-2012, 2012.

Mehrbach, C., Culberson, C. H., Hawley, J. E., and Pytkowicz, R. M.: Measurement of the apparent dissociation constants of carbonic acid in seawater at atmospheric pressure, Limnol. Oceanogr., 18, 897–907, 1973.

Nicolsky, D. J., Romanovsky, V. E., Romanovskii, N. N., Kholodov, A. L., Shakhova, N. E., and Semiletov, I. P.: Modeling sub-sea permafrost in the East Siberian Arctic Shelf: the Laptev Sea region, J. Geophys. Res., 117, F03028, doi:10.1029/2012JF002358, 2012.

Pavlova, G. Yu., Tishchenko, P. Ya., Volkova, T. I., Dickson, A., and Wallmann, K.: Intercalibration of Bruevich's method to determine the total alkalinity in seawater, Oceanology, 48, 460–465, 2008.

Petelin, V. P.: New method of water-mechanical analyze of marine bottom sediment, Oceanology, 1, 143–148, 1961 (in Russian).

Pipko, I. I., Semiletov, I. P., and Pugach, S. P.: The carbonate system of the East Siberian Sea waters, Dokl. Earth Sci., 402, 624–627, 2005.

Pipko, I. I., Pugach, S. P., Dudarev, O. V., Charkin, A. N., and Semiletov, I. P.: Carbonate parameters of the Lena River: characteristics and distribution, Geochem. Int., 48, 1131–1137, 2010.

Pipko, I. I., Semiletov, I. P., Pugach, S. P., Wåhlström, I., and Anderson, L. G.: Interannual variability of air-sea CO_2 fluxes and carbon system in the East Siberian Sea, Biogeosciences, 8, 1987–2007, doi:10.5194/bg-8-1987-2011, 2011.

Proshutinsky, A. Y. and Johnson, M. A.: Two circulation regimes of the wind-driven Arctic Ocean, J. Geophys. Res., 102, 12493–12514, 1997.

Pugach, S. P. and Pipko, I. I.: Dynamics of colored dissolved organic matter on the East Siberian Sea shelf, Dokl. Earth Sci., 448, Part 1, 153–156, 2013.

Rachold, V., Grigoriev, M. N., Are, F. E., Solomon, S., Reimnnitz, E., Kassens, H., and Antonow, M.: Coastal erosion vs. riverine sediment discharge in the Arctic shelf seas, Int. J. Earth Sci., 89, 450–460, 2000.

Rachold, V., Eicken, H., Gordeev, V., Grigoriev, M., Hubberten, H., Lisitzin, A., Shevchenko, V., and Schirmeister, L.: Modern terrigenous organic carbon input to the Arctic Ocean, in: The

Organic Carbon Cycle in the Arctic Ocean, edited by: Stein, R. and Macdonald, R. W., Springer-Verlag, Berlin, Heidelberg, New York, 512 pp., 2004.

Sánchez-Garcia, L., Alling, V., Pugach, S., Vonk, J., van Dongen, B., Humborg, C., Dudarev, O., Semiletov, I., and Gustafsson, Ö.: Inventories and behavior of particulate organic carbon in the Laptev and East Siberian seas, Global Biogeochem. Cy., 25, GB2007, doi:10.1029/2010GB003862, 2011.

Savelieva, N. I., Semiletov, I. P., Vasilevskaya, L. N., and Pugach, S. P.: A climate shift in seasonal values of meteorological and hydrological parameters for Northeastern Asia, Prog. Oceanogr., 47, 279–297, 2000.

Semiletov, I. P.: Ancient ice air content of the Vostok Ice Core, in: Biogeochemistry of Trace Gases, edited by: Oremland, S., Chapman and Hall Inc., New York, 46–59, 1993.

Semiletov, I. P.: On aquatic sources and sinks of CO_2 and CH_4 in the polar regions, J. Atmos. Sci., 56, 286–306, 1999a.

Semiletov, I. P.: The failure of coastal frozen rock as an important factor in the biogeochemistry of the arctic shelf water, Dokl. Earth Sci., 369, 1140–1143, 1999b.

Semiletov, I. P. and Pipko, I. I.: Sinks and sources of carbon dioxide in the Arctic Ocean: results of direct instrumental measurements, Dokl. Earth Sci., 414, 642–645, 2007.

Semiletov, I. P., Pipko, I. I., Pivovarov, N. Ya., Popov, V. V., Zimov, S. A., Voropaev, Yu. V., and Daviodov, S. P.: Atmospheric carbon emission from north Asian lakes: A factor of global significance, Atmos. Environ., 30, 1657–1671, 1996.

Semiletov, I. P., Savelieva, N. I., Weller, G. E., Pipko, I. I., Pugach, S. P., Gukov, A. Yu., and Vasilevskaya, L. N.: The dispersion of Siberian river flows into coastal waters: meteorological, hydrological and hydrochemical aspects, in: The Freshwater Budget of the Arctic Ocean, NATO Meeting/NATO ASI Series, edited by: Lewis, E. L., Kluwer Academic Publishers, Dordrecht, 323–367, 2000.

Semiletov, I. P., Makshtas, A., Akasofu, S.-I., and Andreas, E.: Atmospheric CO_2 balance: the role of Arctic sea ice, Geophys. Res. Lett., 31, L05121, doi:10.1029/2003GL017996, 2004.

Semiletov, I., Dudarev, O., Luchin, V., Charkin, A., Shin, K., and Tanaka, N.: The East-Siberian Sea as a transition zone between the Pacific origin water and local shelf water, Geophys. Res. Lett., 32, L10614, doi:10.1029/2005GL022490, 2005.

Semiletov, I. P., Pipko, I. I., Repina, I., and Shakhova, N. E.: Carbonate chemistry dynamics and carbon dioxide fluxes across the atmosphere-ice-water interfaces in the Arctic Ocean: Pacific sector of the Arctic, J. Marine Syst., 66, 204–226, 2007.

Carbon dynamics in the Buor-Khaya Bay of the Laptev Sea

I. P. Semiletov et al.

Semiletov, I. P., Pipko, I. I., Shakhova, N. E., Dudarev, O. V., Pugach, S. P., Charkin, A. N., McRoy, C. P., Kosmach, D., and Gustafsson, Ö.: Carbon transport by the Lena River from its headwaters to the Arctic Ocean, with emphasis on fluvial input of terrestrial particulate organic carbon vs. carbon transport by coastal erosion, Biogeosciences, 8, 2407–2426, doi:10.5194/bg-8-2407-2011, 2011.

Semiletov, I. P., Shakhova, N. E., Sergienko, V. I., Pipko, I. I., and Dudarev, O. V.: On carbon transport and fate in the East Siberian Arctic land-shelf-atmosphere system, Environ. Res. Let., 7, 015201, doi:10.1088/1748-9326/7/1/015201, 2012.

Shakhova, N. E. and Semiletov, I. P.: Characteristic features of carbon cycle in the shallow shelf of the eastern sector of Russian Arctic, in: Environmental and Climate Changes and Catastrophes, Vol. 4, edited by: Laverov, N. P., Institute of Physicochemical and Biological Problems of Soil Science, Russian Academy of Sciences, Moscow, 167–181, 2008.

Shakhova, N., Semiletov, I., Leifer, I., Rekant, P., Salyuk, A., and Kosmach, D.: Geochemical and geophysical evidence of methane release from the inner East Siberian Shelf, J. Geophys. Res., 115, C08007, doi:10.1029/2009JC005602, 2010a.

Shakhova, N., Semiletov, I., Salyuk, A., Yusupov, V., Kosmach, D., and Gustafsson, Ö.: Extensive methane venting to the atmosphere from sediments of the East Siberian Arctic Shelf, Science, 327, 1246–1250, 2010b.

Shepard, F. P.: Nomenclature based on sand-silt-clay ratios, J. Sediment. Petrol., 24, 151–158, 1954.

Soloviev, V. A., Ginzburg, G. D., Telepnev, E. B., and Mihalyuk, Yu. N.: Cryothermia and natural gas hydrates within the Arctic Ocean, Sevmorgeologiya, Leningrad, 150 pp., 1987 (in Russian).

Sondergaard, M. and Middelboe, M.: A cross-system analysis of labile dissolved organic carbon, Mar. Ecol.-Prog. Ser., 118, 283–294, 1995.

Sorokin, Yu. A. and Sorokin, P. Yu.: Plankton and primary production in the Lena River estuary and in the South-eastern Laptev Sea, Estuar. Coast. Shelf Sci., 43, 399–418, 1996.

Stein, R. and Macdonald, R. W.: The Organic Carbon Cycle in the Arctic Ocean, Springer-Verlag, Berlin, 417 pp., 2004.

Tarnocai, C., Canadell, J. G., Schuur, E. A. G., Kuhry, P., Mazhitova, G., and Zimov, S.: Soil organic carbon pools in the northern circumpolar permafrost region, Global Biogeochem. Cy., 23, GB2023, doi:10.1029/2008GB003327, 2009.

Title Page

Abstract | Introduction

Conclusions | References

Tables | Figures

|◀ | ▶|

◀ | ▶

Back | Close

Full Screen / Esc

Printer-friendly Version

Interactive Discussion

Vonk, J. E., Sánchez-García, L., Semiletov, I., Dudarev, O., Eglinton, T., Andersson, A., and Gustafsson, Ö.: Molecular and radiocarbon constraints on sources and degradation of terrestrial organic carbon along the Kolyma paleoriver transect, East Siberian Sea, Biogeosciences, 7, 3153–3166, doi:10.5194/bg-7-3153-2010, 2010.

5　Vonk, J. E., Sánchez-García, L., van Dongen, B. E., Alling, V., Kosmach, D., Charkin, A., Semiletov, I. P., Dudarev, O. V., Shakhova, N., Roos, P., Eglinton, T. I., Andersson, A. and Gustafsson, Ö.: Activation of old carbon by erosion of coastal and subsea permafrost in Arctic Siberia, Nature, 489, 137–140, 2012.

Walsh, J. J., McRoy, C. P., Coachman, L. K., Goering, J. J., Nihoul, J. J., Whitledge, T. E., 10　Blackburn, T. H., Parker, P. L., Wirick, C. D., Shuert, P. G., Grebmeier, J. M., Springer, A. M., Tripp, R. D., Hansell, D. A., Djenidi, S., Deleersnijder, E., Henriksen, K., Lund, B. A., Andersen, P., Muller-Karger, F. E., and Dean, K.: Carbon and nitrogen cycling within the Bering/Chukchi Seas: source regions for organic matter effecting AOU demands of the Arctic Ocean, Prog. Oceanogr., 22, 277–359, 1989.

15　Weiss, R. F.: The solubility of nitrogen, oxygen and argon in water and seawater, Deep-Sea Res., 17, 721–735, 1970.

Weiss, R. F.: Determination of gas carbon dioxide and methane by duel catalyst flame ionization chromatography and nitrous oxide by electron capture chromatography, J. Chromatogr. Sci., 19, 611–616, 1981.

20　Wiegner, T. N. and Seitzinger, S. P.: Photochemical and microbial degradation of external dissolved organic matter inputs to rivers, Aquat. Microb. Ecol., 24, 27–40, 2001.

Zimov, S. A., Semiletov, I. P., Daviodov, S. P., Voropaev, Yu. V., Prosyannikov, S. F., Wong, C. S., and Chan, Y.-H.: Wintertime CO_2 emission from soils of Northeastern Siberia, Arctic, 46, 197–204, 1993.

25　Zimov, S. A., Voropaev, Yu. V., Semiletov, I. P., Daviodov, S. P., Chapin, F. S., and Trumbore, S.: North Siberian lakes: a methane source fueled by Pleistocene carbon, Science, 277, 800–802, 1997.

Title Page

Abstract　Introduction

Conclusions　References

Tables　Figures

◀︎　▶︎

◀　▶

Back　Close

Full Screen / Esc

Printer-friendly Version

Interactive Discussion

Table 1. List of summer cruises and winter expeditions (1999–2011).

Cruise	Date
Dunay 1999	9 Sep to 24 Sep
Nikolay Kolomeitsev 2000	30 Aug to 5 Sep
Winter surveys 2002	15 Apr to 4 May
Ivan Kireev 2004	24 Aug to 1 Sep
	14 Sep
Neptun 2005	3 Sep to 8 Sep
Auga 2005	21 Sep to 25 Sep
Neptun 2006	5 Sep to 27 Sep
Winter surveys 2007	3 Apr to 13 Apr
Yakob Smirnitskiy 2008	23 Aug to 29 Aug
	16 Sep to 18 Sep
TB-0012 2008	14 Aug to 26 Aug
TB-0012 2009	25 Aug to 7 Sep
TB-0012 2010	24 Aug to 28 Aug
Akademic Lavrentiev 2011	18 Sep to 30 Sep

Table 2. Correlation matrix of the environmental parameters observed in the BKB in 2005 ($N = 43$).

	T	S	Alk	pH	pCO$_2$	O$_2$	PO$_4^{3-}$	Si	NO$_3^-$	NH$_4^+$	CDOM	POC	PM
T	**1**												
S	−0.97	**1**											
Alk	−0.97	0.99	**1**										
pH	0.74	−0.82	−0.84	**1**									
pCO$_2$	−0.69	0.77	0.80	−0.98	**1**								
O$_2$	0.82	−0.88	−0.90	0.98	−0.97	**1**							
PO$_4^{3-}$	−0.91	0.88	0.88	−0.62	0.53	−0.70	**1**						
Si	0.09	−0.07	0.00	−0.38	0.38	−0.30	−0.04	**1**					
NO$_3^-$	−0.93	0.93	0.95	−0.82	0.75	−0.87	0.92	0.18	**1**				
NH$_4^+$	−0.02	0.01	0.02	−0.14	0.11	−0.12	0.10	0.21	0.17	**1**			
CDOM	0.89	−0.91	−0.87	0.66	−0.59	0.71	−0.75	0.37	−0.76	0.06	**1**		
POC	0.27	−0.26	−0.31	0.11	−0.09	0.18	−0.44	−0.08	−0.37	0.20	0.05	**1**	
SPM	−0.16	0.16	0.12	−0.22	0.26	−0.19	−0.03	−0.14	0.07	−0.02	−0.27	0.70	**1**

Discussion Paper | Discussion Paper | Discussion Paper | Discussion Paper | Discussion Paper

BGD

10, 2159–2204, 2013

Carbon dynamics in the Buor-Khaya Bay of the Laptev Sea

I. P. Semiletov et al.

Title Page

Abstract | Introduction

Conclusions | References

Tables | Figures

|◄ | ►|

◄ | ►

Back | Close

Full Screen / Esc

Printer-friendly Version

Interactive Discussion

Table 3. Correlation matrix of the environmental parameters observed in the BKB in 2011 ($N = 74$).

	T	S	Alk	pH	$p\text{CO}_2$	O_2	PO_4^{3-}	Si	NO_3^-	NH_4^+	CDOM	PM
T	**1**											
S	−0.26	**1**										
Alk	−0.33	0.99	**1**									
pH	0.31	−0.43	−0.42	**1**								
$p\text{CO}_2$	−0.42	0.81	0.82	−0.81	**1**							
O_2	0.35	−0.93	−0.94	0.61	−0.92	**1**						
PO_4^{3-}	−0.48	0.72	0.74	−0.61	0.83	−0.84	**1**					
Si	−0.22	−0.62	−0.58	−0.26	−0.16	0.44	−0.23	**1**				
NO_3^-	−0.68	0.71	0.75	−0.73	0.91	−0.84	0.85	−0.02	**1**			
NH_4^+	−0.06	−0.18	−0.21	−0.31	0.08	0.06	0.12	0.36	0.08	**1**		
CDOM	0.10	−0.91	−0.88	0.24	−0.63	0.79	−0.60	0.73	−0.53	0.28	**1**	
SPM	−0.32	0.27	0.25	−0.33	0.36	−0.33	0.46	−0.04	0.33	0.30	−0.15	**1**
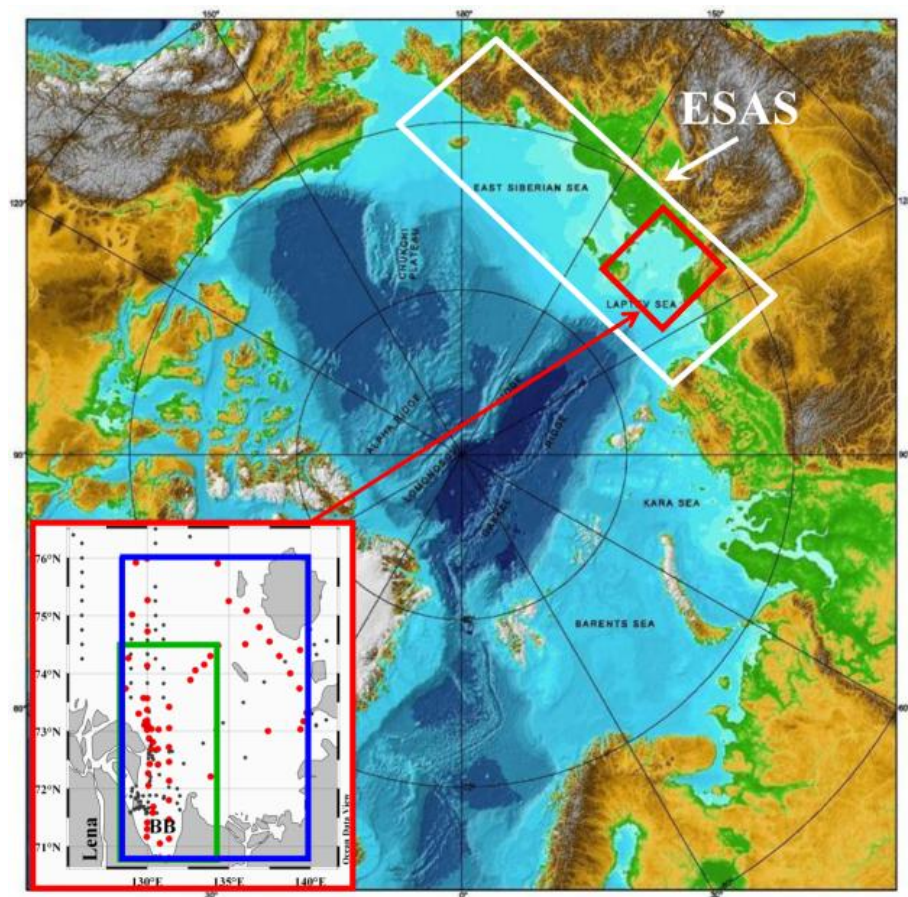
Fig. 1. Study area: position of the BKB of the Laptev Sea in the ESAS. Study area coverage with oceanological stations is shown in the lower left corner.
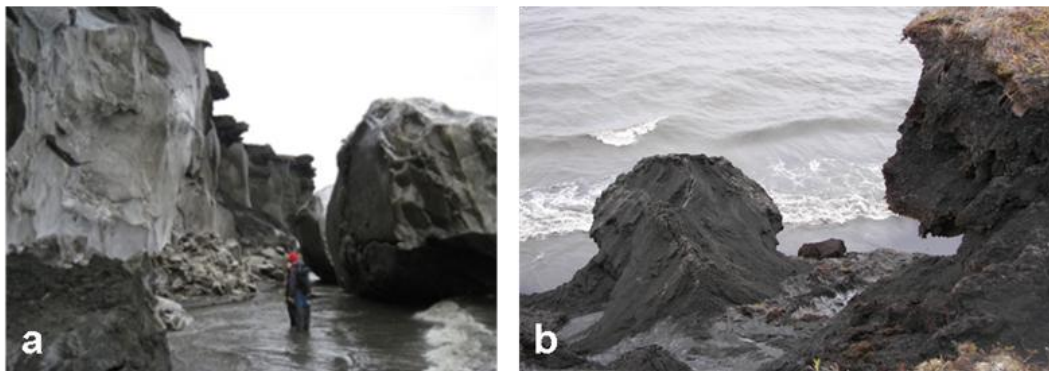
Fig. 2. Coastal erosion as seen on the northern cape of Muostakh Island (photos by I. P. Semiletov). During < 2 weeks in early September 2006, the North Cape of Muostakh Island (Buor-Khaya Gulf of the Laptev Sea) retreated > 20 m delivering a large amount of eroded OC to the sea.
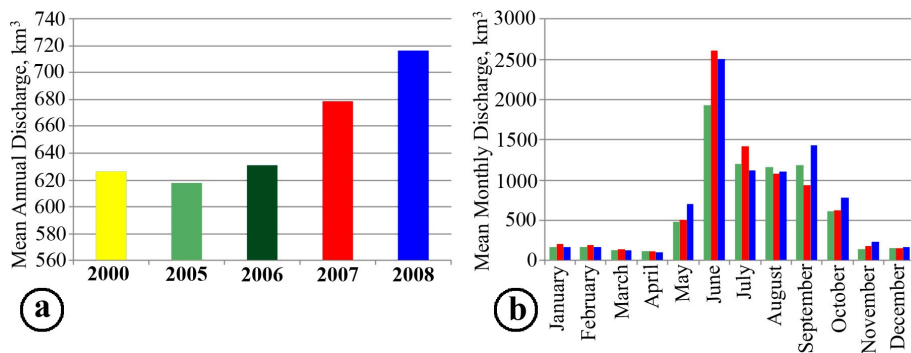
Fig. 3. Mean annual **(a)** and average monthly **(b)** Lena River discharge (Kusur observation station) documented during the period of BKB observations.
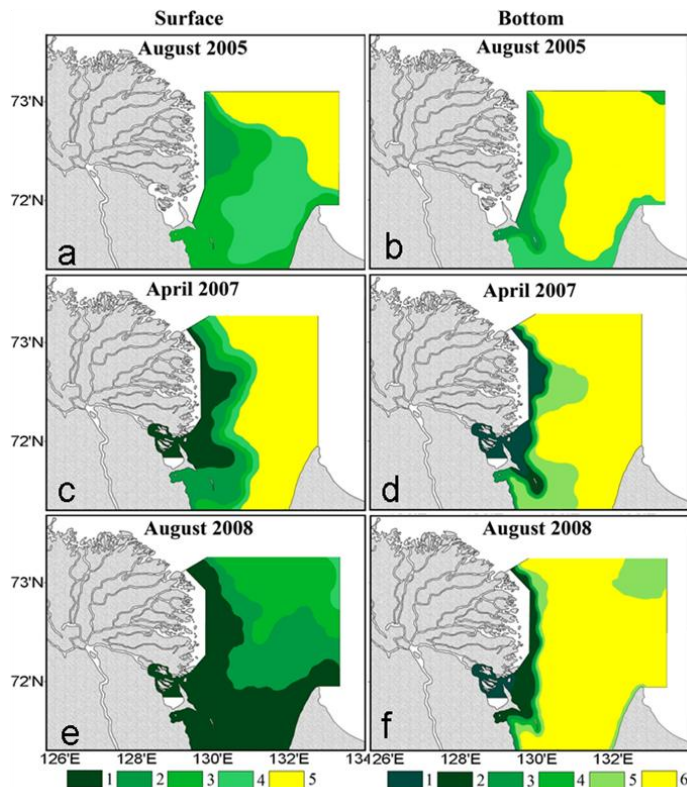
Fig. 4. Salinity of the surface and bottom BKB water layers. Salinity levels shown as colored rectangles below panels **(e)** and **(f)**. For the surface layer: (1) 0–2.5, (2) 2.5–5, (3) 5–7.5, (4) 7.5–10, (5) > 10. For the bottom layer: (1) 0–5, (2) 5–10, (3) 10–15, (4) 15–20, (5) 20–25, (6) > 25.
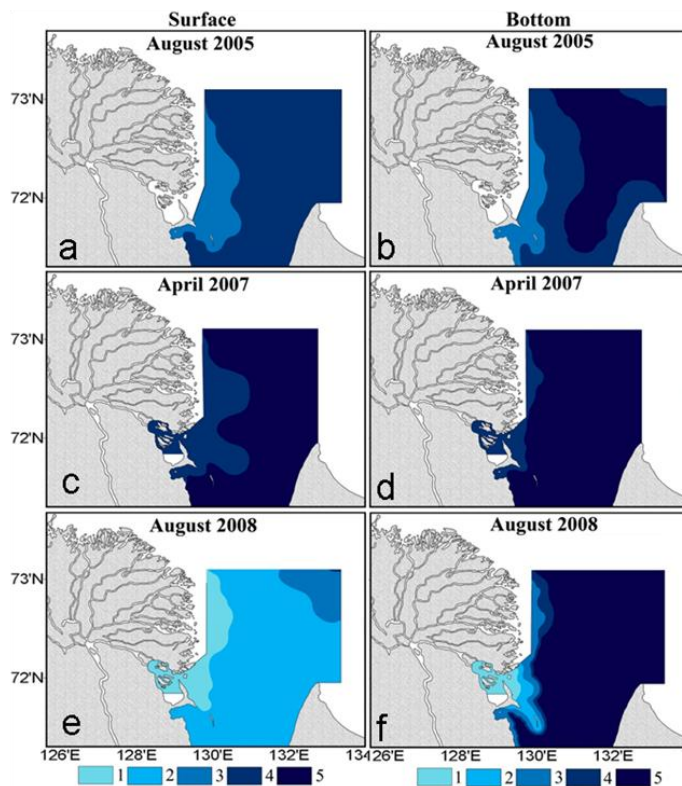
Fig. 5. Temperature of the surface and bottom BKB water layers. Temperature levels (°C) shown as colored rectangles below panels **(e)** and **(f)**. For the surface layer: (1) > 15, (2) 15–10, (3) 10–5, (4) 5–0, (5) < 0. For the bottom layer: (1) > 7.5, (2) 7.5–5, (3) 5–2.5, (4) 2.5–0, (5) < 0.
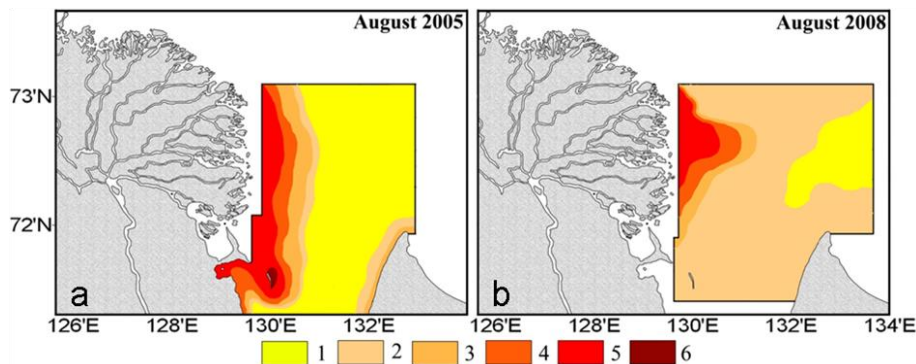
Fig. 6. Distribution of POC in the BKB surface water layer. Concentration range is shown as colored rectangles below the panels (mg L^{-1}): (1) < 0.25, (2) 0.25–0.5, (3) 0.5–0.75, (4) 0.75–1, (5) 1–1.25, (6) > 1.25.

Full Screen / Esc

Printer-friendly Version

Interactive Discussion
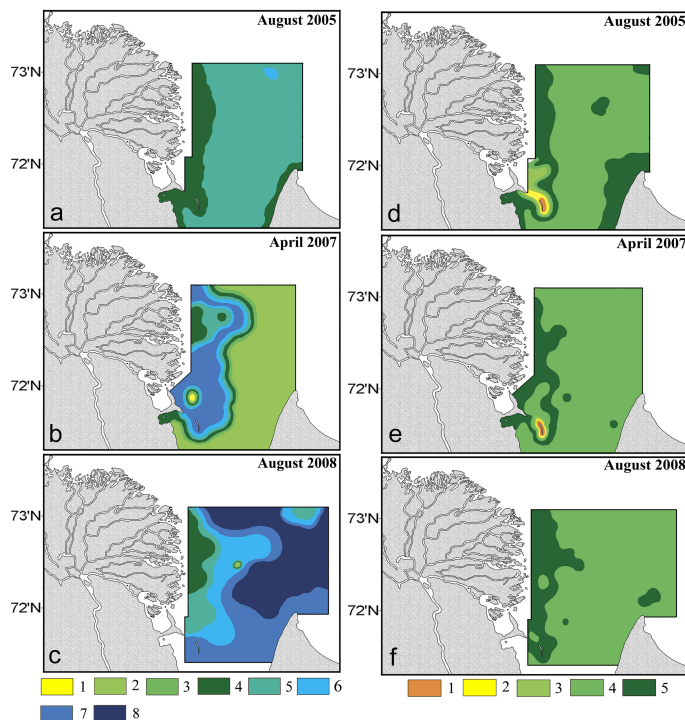
Fig. 7. Inter-annual variability of δ^{13}C of POC observed in BKB sea water **(a–c)** and surface sediments **(d–f)**. Observed value ranges (‰) are shown as colored rectangles below the correspondent panels. For **(a–c)** panels: (1) > (−24), (2) (−24)–(−25), (3) (−25)–(−26), (4) (−26)–(−27), (5) (−27)–(−28), 6) (−28)–(−29), 7) (−29)–(−30), 8) < (−30); for **(d–f)** panels: (1) (−22)–(−23), (2) (−23)–(−24), (3) (−24)–(−25), (4) (−25)–(−26), (5) (−26)–(−27).
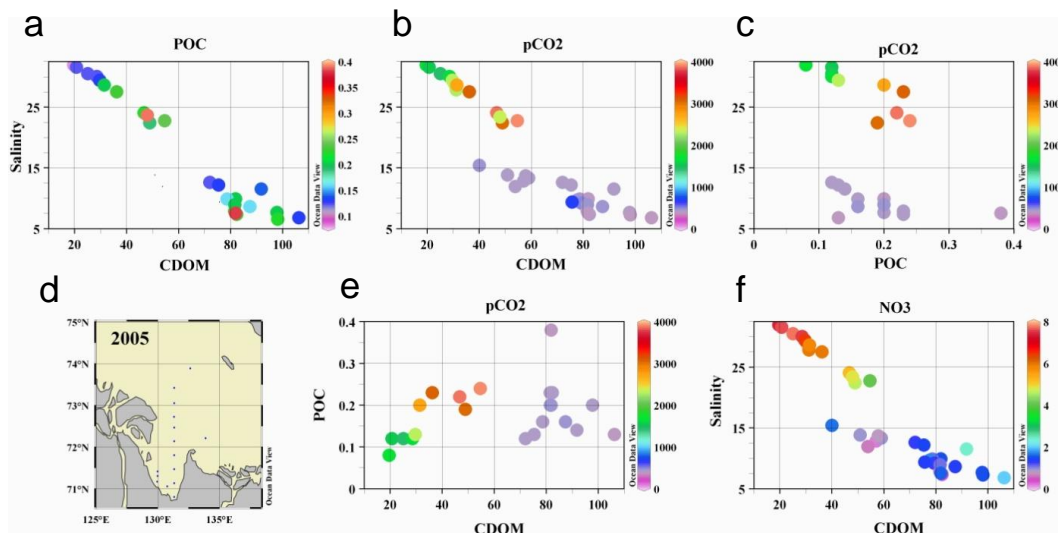
Fig. 8. Plots of POC, mg L^{-1} **(a)** and pCO$_2$, µatm **(b)** color coded by salinity and CDOM; pCO$_2$ color coded by POC **(c)** and CDOM **(e)**; NO$_3^-$, µM color coded by salinity and CDOM **(f)**. Position of the transect conducted in September 2005 is shown in panel **(d)**.
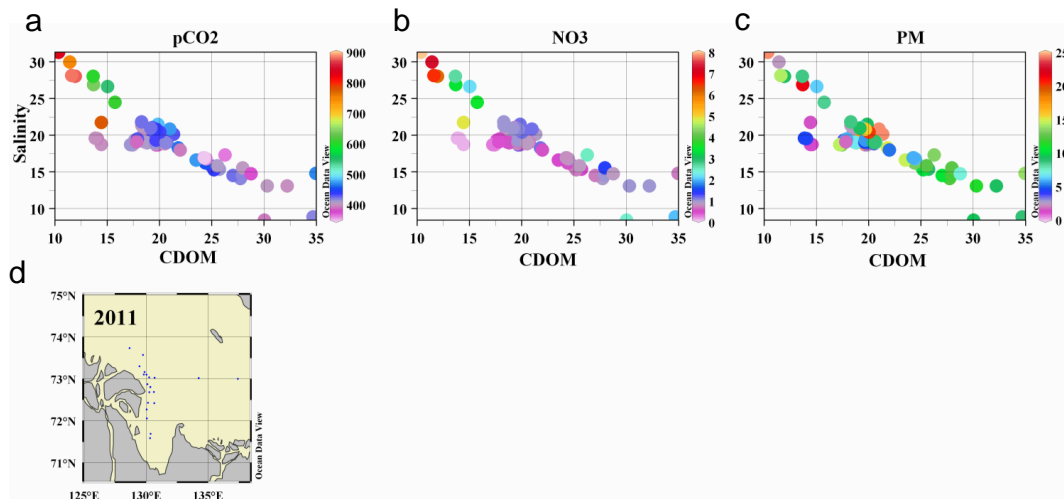
Fig. 9. Plots of pCO_2, µatm, color coded by salinity and CDOM, $mg\,m^{-3}$ **(a)**; NO_3^- (µM) color coded by salinity and CDOM **(b)**; SPM ($mg\,L^{-1}$) color coded by salinity and CDOM **(c)**. Position of transect performed in 2011 is shown in panel **(d)**.
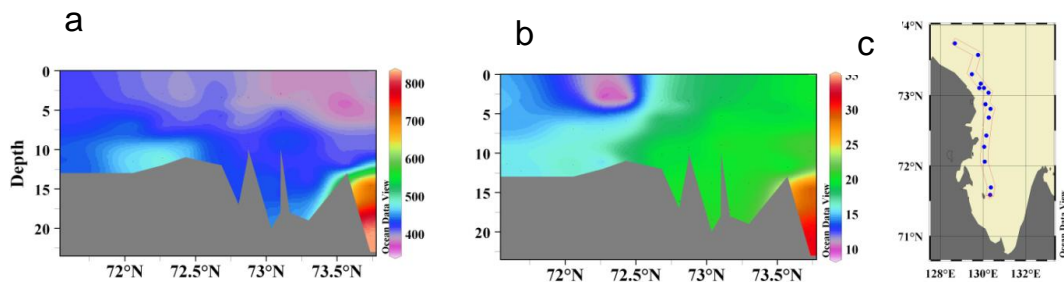
Fig. 10. Distribution of pCO$_2$, µatm **(a)** and salinity **(b)** in the water column of the BKB along the transect observed in 2011. Position of transect is shown in panel **(c)**.
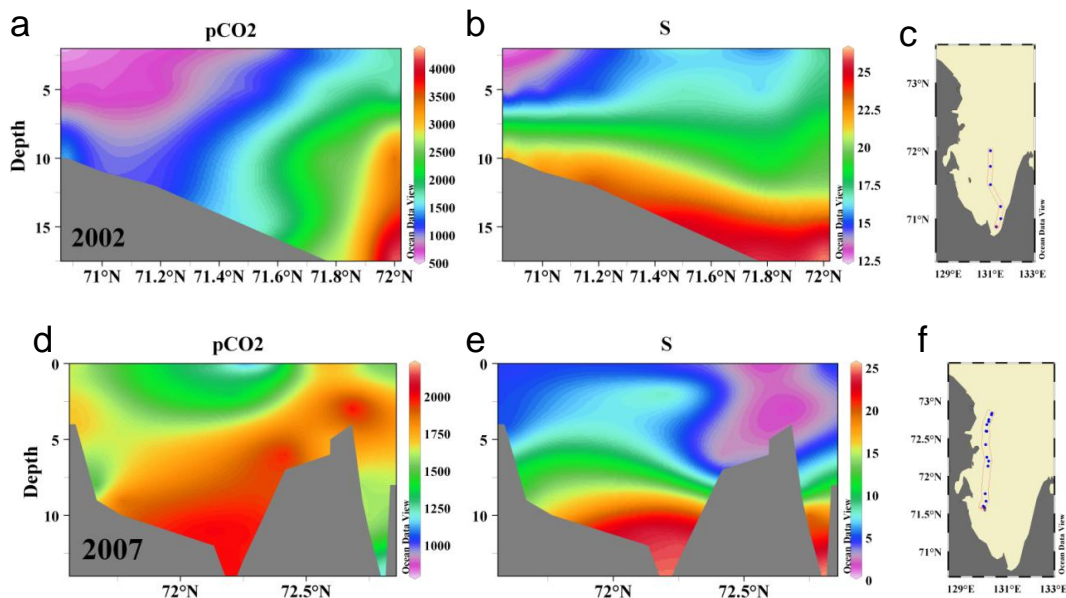
Fig. 11. Vertical distribution of pCO$_2$, µatm (**(a)**, 2002; **(d)**, 2007) and salinity (**(b)**, 2002; **(e)**, 2007) in the water column observed in the BKB in winters 2002 and 2007. Positions of transects are shown in **(c)** (2002) and panel **(f)** (2007).
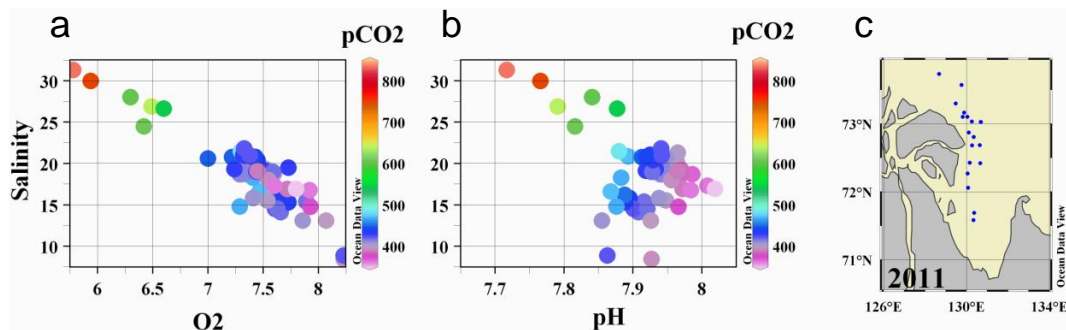
Fig. 12. Plots of pCO_2, µatm, color coded by salinity and O_2, **(a)**; pCO_2 color coded by salinity and pH **(b)**. Position of transects is shown in panel **(c)**.
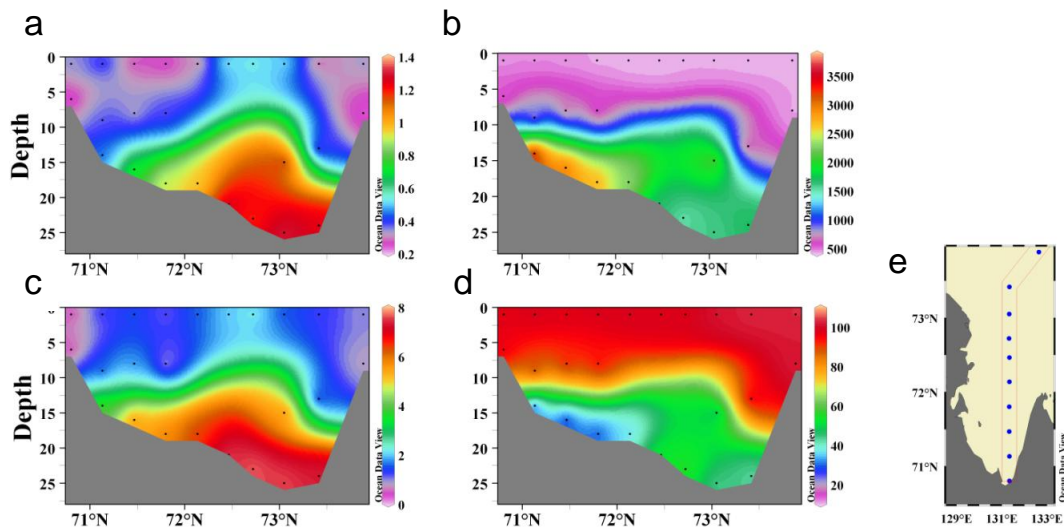
Fig. 13. Vertical distribution of PO_4^{3-}, µM **(a)**, pCO_2, µatm **(b)**, NO_3^- µM **(c)**, and O_2, % **(d)** in the water column observed in the BKB in summer 2005. Transect position is shown in panel **(e)**.
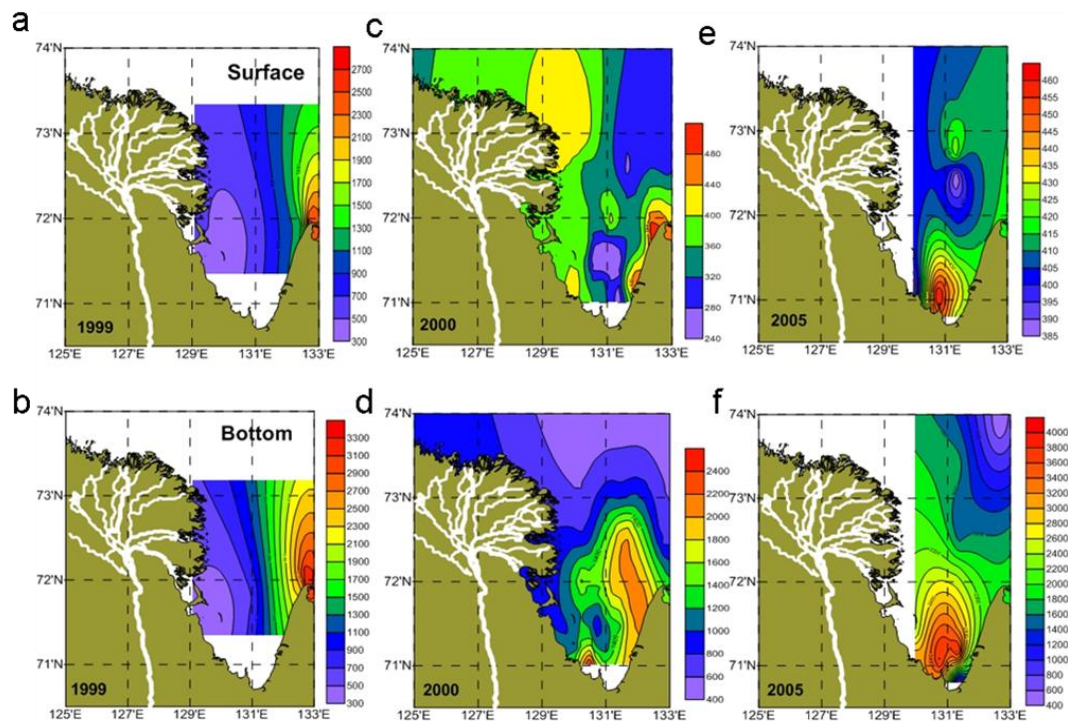
Fig. 14. Distribution of pCO_2 (µatm) in the surface and bottom water layer of the BKB observed in 1999 **(a, b)**, 2000 **(c, d)**, and 2005 **(e, f)**.

Title Page

Abstract | Introduction

Conclusions | References

Tables | Figures

|◄ | ►|

◄ | ►

Back | Close

Full Screen / Esc

Printer-friendly Version

Interactive Discussion
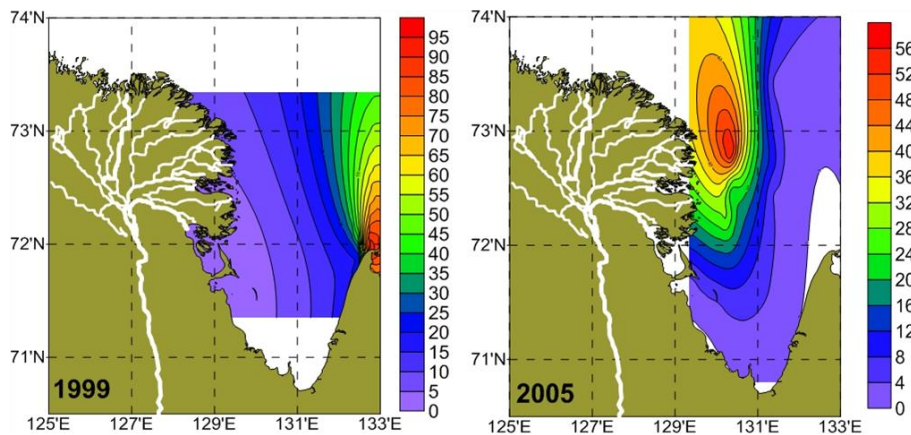
Fig. 15. Distribution of sea-air CO_2 fluxes, F_{CO_2}, $mmol\,m^{-2}\,day^{-1}$ in the BKB observed in September 1999 (left panel) and September 2005 (right panel).
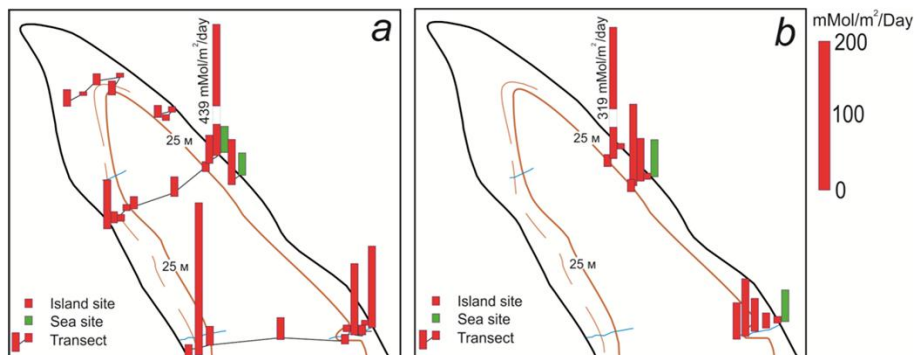
Fig. 16. Distribution of CO_2 outgassing (F_{CO_2}, mmol m^{-2} day^{-1}) from Muostakh Island sites (red columns) and from sea sites (green columns) in September 2006 **(a)**, and in September 2009 **(b)**.